13

Two-Scale Phase Shift Functions

Phase shift functions can of course also have a rich structure without the inclusion of a long-range Coulomb interaction. The present chapter presents two such examples. The first example is simply a superposition of two Gaussians, whereas the second example is defined in terms of the derivative $X'(b_x)$ rather than the phase shift function $X(b_x)$ itself.

13.1 Two Gaussians

We shall here consider the superposition of two concentric Gaussians having however different ranges, $\beta_1 \neq \beta_2$:

$$X(b_x) = A_1 \exp(-b_x^2/\beta_1^2) + A_2 \exp(-b_x^2/\beta_2^2). \tag{13.1}$$

As two explicit examples, we consider

$$X_1(b_x) = 5\exp[-(b_x/\beta_1)^2] + 3\exp[-(b_x/\beta_2)^2], \tag{13.2a}$$

$$X_2(b_x) = 5\exp[-(b_x/\beta_1)^2] - 3\exp[-(b_x/\beta_2)^2], \tag{13.2b}$$

with $\beta_1 = 1$ fm and $\beta_2 = 2$ fm. These phase shift functions, and their first derivatives, are shown in Figs. 13.1 and 13.2, respectively. The first form, Eq. (13.2a), is attractive throughout, whereas the second form, Eq. (13.2b) has a long-range part corresponding to repulsion.

The corresponding maps of regions in the complex b_x-plane, where $\mathrm{Re}\, X'(b_x)$ is respectively positive and negative, are shown in Figs. 13.3 and 13.4 for the two phase shift functions. Together with the contours where $\mathrm{Im}\, X'(b_x) = 0$, these reveal where points of stationary phase may occur. For the present phase shift functions, these maps have a very rich and complicated pattern in the region close to the imaginary axis. This is due to the interplay of the two Gaussians, each of which becomes singular for $b_x \to \pm i \cdot \infty$.

Downloaded from https://www.cambridge.org/core. UNIVERSIDAD AUTONOMA METROPOLITANA, on 12 Nov 2026 at 08:29:50, subject to the Cambridge Core terms of use, available at https://www.cambridge.org/core/terms. https://doi.org/10.1017/9781316219256.017

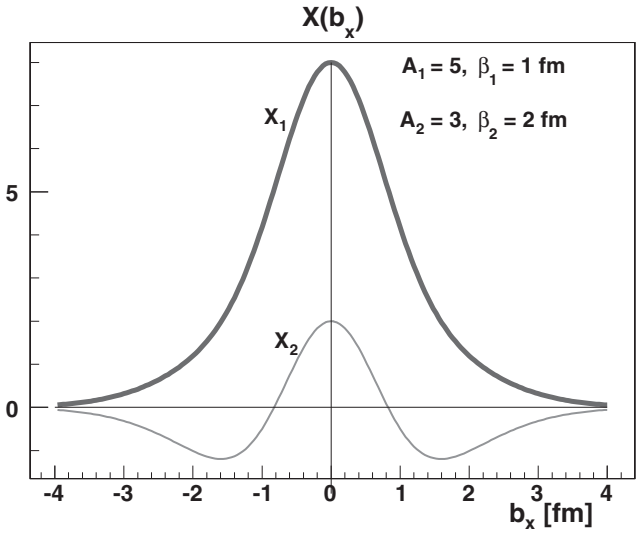


Figure 13.1 The double-Gaussian phase shift functions Eq. (13.2).

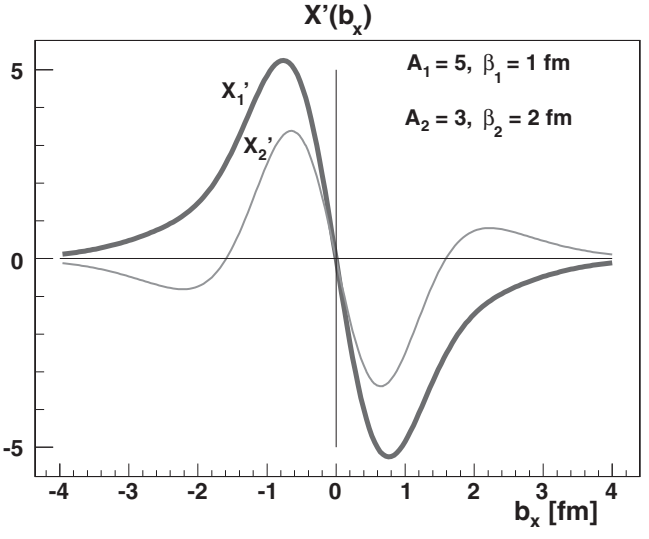


Figure 13.2 Derivatives of the double-Gaussian phase shift functions Eq. (13.2).

We shall discuss in some detail the second of these phase shift functions, Eq. (13.2b), which leads to two rainbow points and in that sense has a richer structure. For the parameters adopted in Figs. 13.1, 13.2, and 13.4, the rainbow points occur at ($b_{\mathrm{R1}} = 2.22$ fm, $q_{\mathrm{R1}} = 0.16$ GeV/c) and ($b_{\mathrm{R2}} = -0.65$ fm, $q_{\mathrm{R2}} = 0.67$ GeV/c). The lower rainbow point, at positive b_x, can be associated with the

Downloaded from https://www.cambridge.org/core. UNIVERSIDAD AUTONOMA METROPOLITANA, on 12 Nov 2026 at 08:29:50, subject to the Cambridge Core terms of use , available at https://www.cambridge.org/core/terms. https://doi.org/10.1017/9781316219256.017

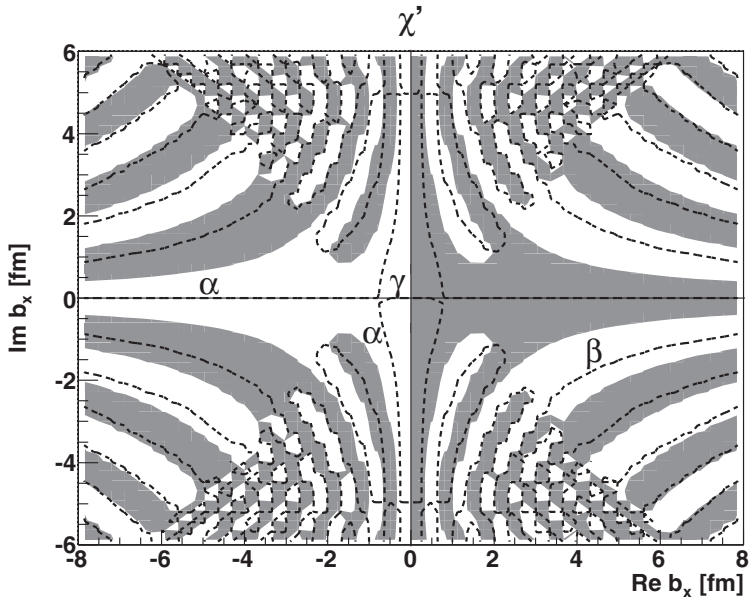


Figure 13.3 Regions of positive (white) and negative (shaded) values of $\mathrm{Re}\, X'(b_x)$, shown in the complex b_x-plane for the double-Gaussian phase shift function Eq. (13.2a).

long-range repulsion, whereas the higher one, at negative b_x, is to a large extent determined by the short-range attractive part of the interaction. It has an analogue at a similar value of b_{R} for the all-attractive phase shift function Eq. (13.2a).

The following question arises: For this case of a rainbow singularity at $b_x = b_{\mathrm{R}2} < 0$, how does the path of integration enter from $\mathrm{Re}\, b_x = -\infty$? In particular, is there any additional point of stationary phase further out, as appears quite possible from the map shown in Fig. 13.4? In other words, does the valley coming in from $\mathrm{Re}\, b_x = -\infty$ pass through the shaded region (in which case there is no further point of stationary phase) or not? This question can easily be answered by studying $|\exp[-iqb_x + iX(b_x)]|$ in the complex b_x plane, a further point of stationary phase is encountered. The corresponding point of stationary phase will be referred to as ϵ, but its contribution to the scattering amplitude is not quantitatively significant.

The differential cross section resulting from this phase shift function Eq. (13.2b) has in the region of the rainbow singularities a rich structure, as illustrated in Fig. 13.5. Inside the first rainbow point, $q < q_{\mathrm{R}1}$, there are contributions from four points of stationary phase on the real axis, denoted as α, β, γ, and δ, plus one below the real axis, in the third quadrant, denoted ϵ. The contribution from β (at large positive b_x, corresponding to the repulsive interaction) is the dominant one. At the rainbow point, it diverges, as does the contribution from δ.

Downloaded from https://www.cambridge.org/core. UNIVERSIDAD AUTONOMA METROPOLITANA, on 12 Nov 2026 at 08:29:50, subject to the Cambridge Core terms of use, available at https://www.cambridge.org/core/terms. https://doi.org/10.1017/9781316219256.017

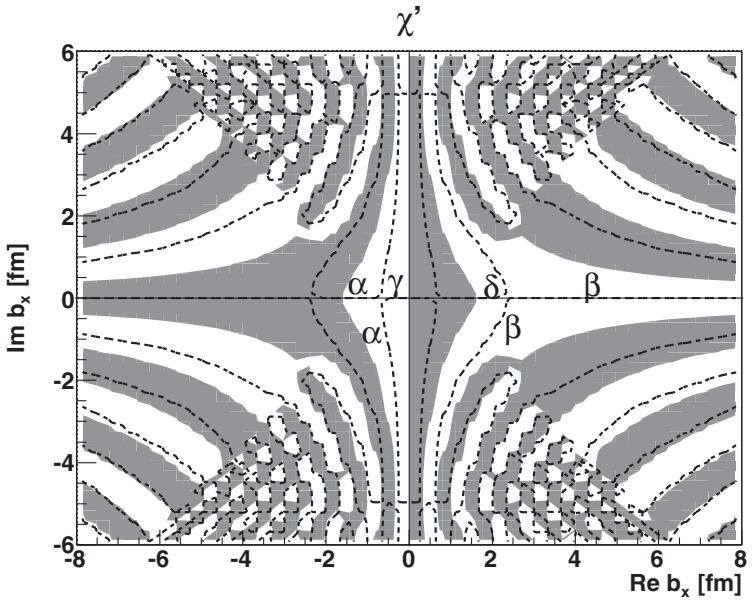


Figure 13.4 Regions of positive (white) and negative (shaded) values of Re X' (b_x), shown in the complex b_x-plane for the double-Gaussian phase shift function Eq. (13.2b).

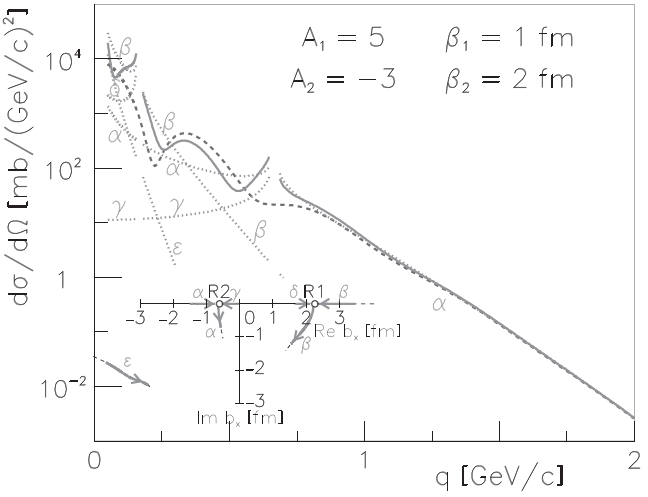


Figure 13.5 Differential cross section for the phase shift function Eq. (13.2b). The inserts show the trajectories of stationary points for 0.02 GeV/c $\leq q \leq$ 5.0 GeV/c (dotted). The parts that correspond to the cross section plots, 0.05 GeV/c $\leq q \leq$ 2.0 GeV/c are shown as solid curves. The cross sections contributed by the individual stationary points, are shown as dotted curves. The solid curves give the resulting interference pattern. The heavy dashed curve represents the result of direct numerical integration.

Downloaded from https://www.cambridge.org/core. UNIVERSIDAD AUTONOMA METROPOLITANA, on 12 Nov 2026 at 08:29:50, subject to the Cambridge Core terms of use , available at https://www.cambridge.org/core/terms. https://doi.org/10.1017/9781316219256.017

Then, between the two rainbows, there are three contributions. In the first part of this interval, it is the β-contribution which continues to dominate, while in the outer part of the interval, as $q \to q_{R2}$, the contributions from α and γ dominate and eventually become singular. An oscillatory pattern develops, due to these different contributions having different dependencies on q.

Outside the second rainbow, the differential cross section has a smooth falloff, with contributions from β and α, the latter being dominant. Again we see that in the region of the rainbows, the agreement is not very good. As discussed above, both the asymptotic approach and the numerical one have difficulties here, for different reasons.

13.2 The "Shoulder Function"—Three Rainbows

If the derivative of the phase shift function has two positive maxima, $X'(b_x) > 0$, there will be two rainbow points, as we have seen illustrated in various cases. It is interesting to study what happens when also the minimum between these two maxima is *positive*. It is easy to find a phase shift function with this property, if we simply start with $X'(b_x)$, rather than $X(b_x)$. Thus, in analogy with the case studied in Section 10.2.1, we let

$$f(b_x) \equiv -(b_x/\beta_1^2)A_1 \exp(-b_x^2/\beta_1^2) - (b_x^3/\beta_2^4)A_2 \exp(-b_x^2/\beta_2^2), \tag{13.3}$$

and take

$$X'(b_x) = f(b_x). \tag{13.4}$$

For β_1 somewhat smaller than β_2, this function $f(b_x)$ has one maximum controlled mostly by A_1 and the first Gaussian, and a second one further out, in part because of β_2 being larger than β_1, and in part because of the higher power of b_x in front. An even higher (but odd) power could also be considered.

An example is shown in Fig. 13.6, for $A_1 = A_2 = 5$, $\beta_1 = 1$ fm and $\beta_2 = 3$ fm. It is clear that at low momentum transfers there will be two points of the stationary phase on the real axis. As the momentum transfer is increased, at some point q_{R1} there will be a first rainbow. But this rainbow differs from those we have encountered so far in having a *larger* number of stationary points as the momentum transfer is further increased. Immediately beyond this value of momentum transfer, there are four points of stationary phase. Thus, it is clear that for $q < q_{R1}$, there must be three points of stationary phase, one of them off the real axis, in the lower half-plane. With the parameters chosen for Fig. 13.6, the rainbow points occur at $q_{R1} = 0.32$ GeV/c, $q_{R2} = 0.54$ GeV/c and $q_{R3} = 0.86$ GeV/c,

As the momentum transfer is further increased, the remaining two rainbows are encountered, with pairs of stationary points running together at q_{R2} and q_{R3}. This will be illustrated shortly.

Downloaded from https://www.cambridge.org/core. UNIVERSIDAD AUTONOMA METROPOLITANA, on 12 Nov 2026 at 08:29:50, subject to the Cambridge Core terms of use, available at https://www.cambridge.org/core/terms. https://doi.org/10.1017/9781316219256.017

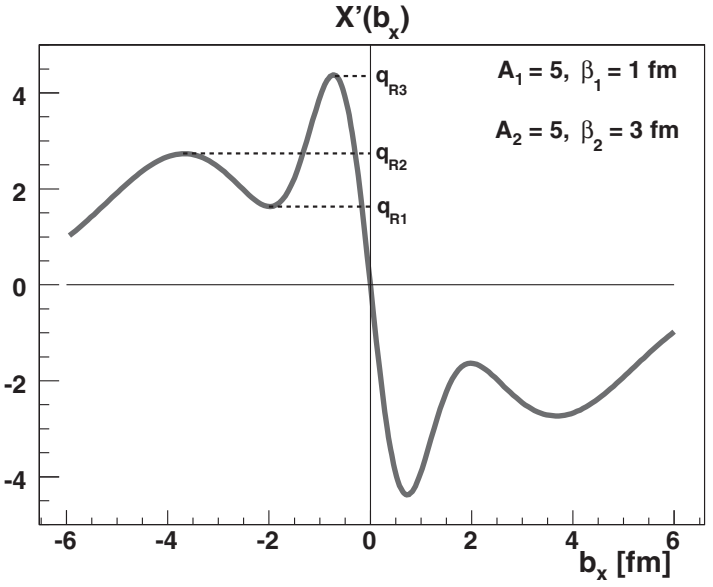


Figure 13.6 The derivative, Eq. (13.4), of a phase shift function yielding three rainbow points, denoted $q_{\mathrm{R}1}$, $q_{\mathrm{R}2}$, and $q_{\mathrm{R}3}$. As the momentum transfer is increased from zero, the number of stationary points along the real axis is seen to go from two to four to two to none. There will be additional points of stationary phase in the complex plane: first one, then two.

In order to calculate the cross section, we need also the phase shift function itself, obtained by integration:

$$X(b_x) = -\int_{b_x}^{\infty} \mathrm{d}t\; X'(t) = -\int_{b_x}^{\infty} \mathrm{d}t\; f(t), \qquad \mathrm{Re}\, b_x > 0,$$
$$X(-b_x) = X(b_x). \tag{13.5}$$

This procedure is completely analogous to the case studied in Section 10.2.1. The result is shown in Fig. 13.7 for real values of b_x. We shall refer to this function as a "shoulder function."

The differential cross section, shown in Fig. 13.8, is in this case not so well reproduced by the asymptotic approximation. This is actually to be expected, due to the fact that the rainbow singularities are relatively near each other. Approximating the contribution of each point of stationary phase by a Gaussian integral from minus infinity to plus infinity then becomes inaccurate. However, there is an interesting new feature. The lowest-lying rainbow point, at $(b_{\mathrm{R}1}, q_{\mathrm{R}1})$, and labeled "R1" in the figure, has the property that for $q < q_{\mathrm{R}1}$, there is only one contribution associated with it, from the point of stationary phase γ, located off the real axis, in the lower half-plane. Beyond it, for $q > q_{\mathrm{R}1}$, there are two contributions, from the points of stationary phase γ and δ, both on the real axis.

Downloaded from https://www.cambridge.org/core. UNIVERSIDAD AUTONOMA METROPOLITANA, on 12 Nov 2026 at 08:29:50, subject to the Cambridge Core terms of use , available at https://www.cambridge.org/core/terms. https://doi.org/10.1017/9781316219256.017

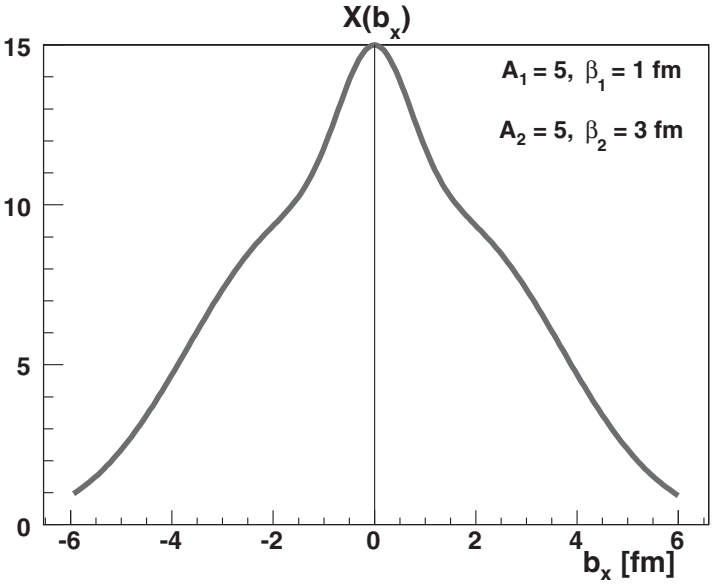


Figure 13.7 The phase shift function corresponding to the derivative given by Eq. (13.4).

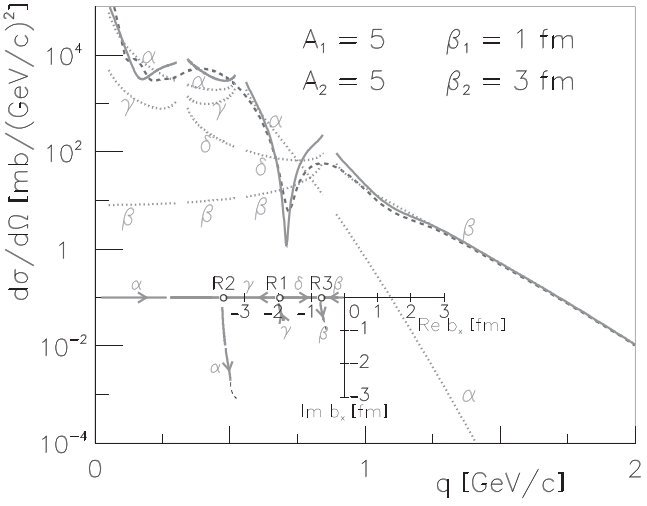


Figure 13.8 Differential cross sections corresponding to the real phase shift function whose derivative is given by Eq. (13.4).

For increasing values of the momentum transfer, but in the region $q_{R1} < q < q_{R2}$, these two points of stationary phase, γ and δ, move away from the rainbow point b_{R1}. The next rainbow point occurs at (b_{R2}, q_{R2}), where γ meets α and there ceases to exist, while α then moves into the complex plane. Likewise, δ meets β at

Downloaded from https://www.cambridge.org/core. UNIVERSIDAD AUTONOMA METROPOLITANA, on 12 Nov 2026 at 08:29:50, subject to the Cambridge Core terms of use , available at https://www.cambridge.org/core/terms. https://doi.org/10.1017/9781316219256.017

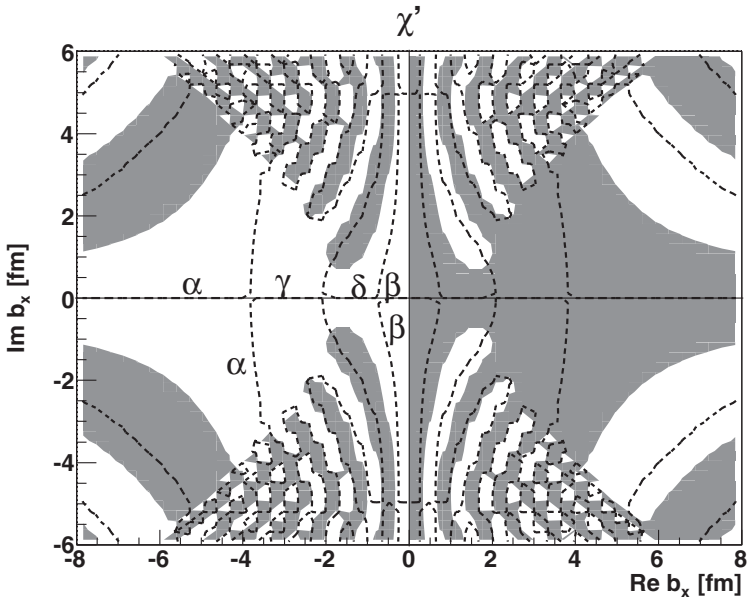


Figure 13.9 Regions of positive and negative values of $\mathrm{Re}\, X'(b_x)$, shown in the complex b_x-plane for the phase shift function whose derivative is given by Eq. (13.4).

the rainbow point $(b_{\mathrm{R3}}, q_{\mathrm{R3}})$ and there ceases to exist. Thus, the point of stationary phase δ only exists for a finite range of momentum transfers.

These possible locations of the stationary points can also be seen from the map in Fig. 13.9. This map has a lot of structure around the imaginary axis, this is due to the Gaussians becoming singular as $\mathrm{Im}\, b_x \to \pm\infty$, and the modulation with a "high" power of b_x.

Another unfamiliar property of the trajectory of stationary points denoted γ becomes clear from an inspection of Fig. 13.9: Whereas trajectories for forward scattering typically start at $\pm\infty$ or 0, the trajectory γ starts at a finite point in the complex b_x-plane, namely where the contour indicating $\mathrm{Im}\, X'(b_x) = 0$ intersects the borderline between the allowed white region (where $\mathrm{Re}\, X'(b_x) > 0$) and the forbidden shaded region (where $\mathrm{Re}\, X'(b_x) < 0$). This is thus a point where both real and imaginary parts of $X'(b_x)$ vanish. It is however not a rainbow point since there are no crossing lines corresponding to $\mathrm{Im}\, X'(b_x) = 0$.

13.3 The Shoulder Function for Absorption

We shall here discuss the absorptive version of the phase shift function defined by its derivative, Eq. (13.4). As we saw for the real case, in Section 13.2, this

Downloaded from https://www.cambridge.org/core. UNIVERSIDAD AUTONOMA METROPOLITANA, on 12 Nov 2026 at 08:29:50, subject to the Cambridge Core terms of use , available at https://www.cambridge.org/core/terms. https://doi.org/10.1017/9781316219256.017

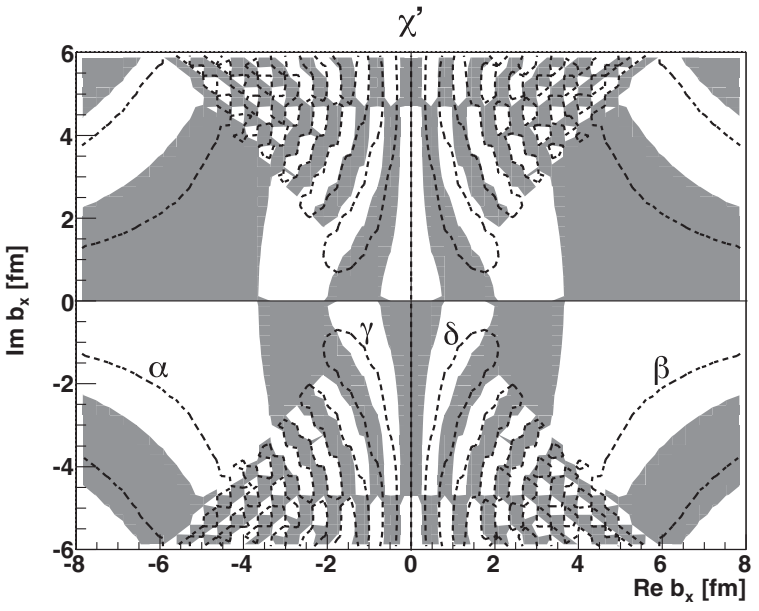


Figure 13.10 Regions of positive and negative values of $\mathrm{Re}\, X'(b_x)$, shown in the complex b_x-plane for the purely imaginary phase shift function whose derivative is given by Eq. (13.4).

functional form can yield a differential cross section with a very rich structure. In the purely imaginary case, as shown in the "map" of Fig. 13.10, there are two pairs of trajectories, one pair associated with each of the two length scales present in Eq. (13.4). As is the case for all purely imaginary phase shift functions, the two points of stationary phase are in each pair related by reflection about the imaginary b_x-axis. In isolation each such pair would thus lead to an oscillatory differential cross section, with an exponentially falling envelope, where the period and slope of the envelope would be determined by the real and imaginary parts of b_x.

Adopting the geometry parameters (β_1 and β_2) of Section 13.2, these two pairs would separately lead to oscillations of rather different periods. This is indeed what happens, as is seen in Fig. 13.11, where we display the cross section out to somewhat larger momentum transfer than was done for the real case.

At moderate momentum transfers, there is a regular pattern resulting from the "outer" points of stationary phase, α and β, mostly determined by the Gaussian with the larger value β_2. The contributions from the stationary points γ and δ are subdominant, since those points are initially further away from the real axis. Eventually, however, these two points of stationary phase, α and β, move further away from the real axis, the contributions from γ and δ become dominant, and the period of oscillation changes dramatically, as does the slope of the envelope.

Downloaded from https://www.cambridge.org/core. UNIVERSIDAD AUTONOMA METROPOLITANA, on 12 Nov 2026 at 08:29:50, subject to the Cambridge Core terms of use , available at https://www.cambridge.org/core/terms. https://doi.org/10.1017/9781316219256.017

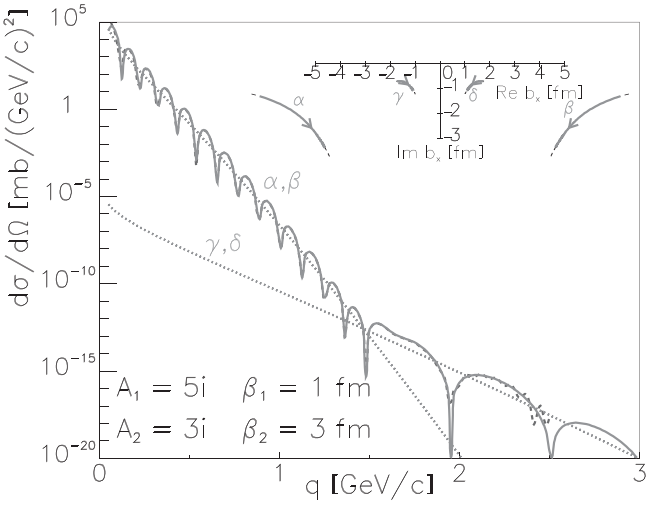


Figure 13.11 Differential cross sections corresponding to the phase shift function whose derivative is given by Eq. (13.4). The inserts show the trajectories of stationary points for $0.02\ \mathrm{GeV/c} \leq q \leq 5.0\ \mathrm{GeV/c}$ (dotted). The parts that correspond to the cross section plots, $0.05\ \mathrm{GeV/c} \leq q \leq 3.0\ \mathrm{GeV/c}$ are shown as solid curves. The cross sections contributed by the individual stationary points, are shown as dotted curves. The solid curve gives the resulting interference pattern. The heavy dashed curve represents the result of the numerical diffraction integral.

In this case, the differential cross section falls by 25 orders of magnitude, and the numerical integration (shown as a heavy dashed curve, practically covered by the solid curve) eventually becomes inaccurate. It is only shown out to $q = 2.5\ \mathrm{GeV/c}$.

Calculations of differential cross sections such as the one we have just presented raise a difficult problem for experimental measurements. We have noted already in Fig. 1.1 that the cross section for proton collisions with ^{208}Pb shows a consistently periodic variation while decreasing over a range of some seven orders of magnitude. It might be natural to assume that extending the measurements to still smaller scattering intensities would reveal nothing new. The cross section in Fig. 13.11, on the other hand, drops by some 17 orders of magnitude before it begins to behave in a radically different way. The drop need not be that dramatic. Altered behavior may intervene at any level.

Downloaded from https://www.cambridge.org/core. UNIVERSIDAD AUTONOMA METROPOLITANA, on 12 Nov 2026 at 08:29:50, subject to the Cambridge Core terms of use , available at https://www.cambridge.org/core/terms. https://doi.org/10.1017/9781316219256.017